ACS central science

Research Article

Cite This: ACS Cent. Sci. 2017, 3, 1096-1102

http://pubs.acs.org/journal/acscii

# A Demonstration of Le Chatelier's Principle on the Nanoscale

Wayne Lin and Catherine J. Murphy*

Department of Chemistry, University of Illinois at Urbana−Champaign, 600 South Mathews Avenue, Urbana, Illinois 61801, United States

Supporting Information

**ABSTRACT:** Photothermal desorption of molecules from plasmonic nanoparticles is an example of a light-triggered molecular release due to heating of the system. However, this phenomenon ought to work only if the molecule−nanoparticle interaction is exothermic in nature. In this study, we compare protein adsorption behavior onto gold nanoparticles for both endothermic and exothermic complexation reactions, and demonstrate that Le Chatelier's principle can be applied to predict protein adsorption or desorption on nanomaterial surfaces. Polyelectrolyte-wrapped gold nanorods were used as adsorption platforms for two different proteins, which we were able to adsorb/desorb from the nanorod surface depending on the thermodynamics of their interactions. Furthermore, we show that the behaviors hold up under more complex biological environments such as fetal bovine serum.

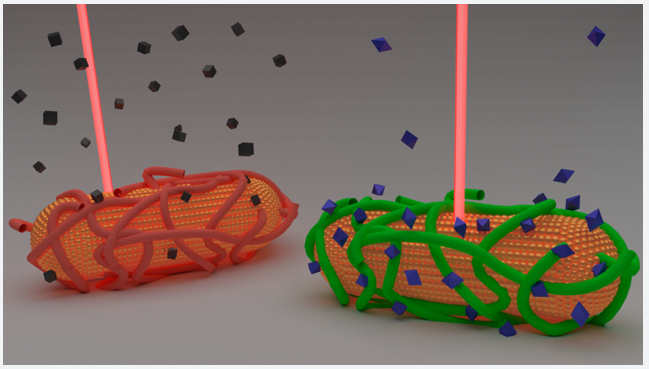



## INTRODUCTION

Gold nanoparticles (Au NPs) have emerged as top candidates for numerous biological applications, such as photothermal therapy and drug delivery, given their relative chemical inertness in biological systems.[1−5] Au NPs offer tunable surface chemistry[6−8] and plasmonic properties that lead to enhanced scattering or rapid heating by tuning NP dimensions and therefore the responsive laser wavelength.[9] The initial surface chemistry of NPs in biological systems is known to be altered by the presence of adventitious proteins.[10−12] Nonetheless, photothermal heating of plasmonic NPs has been used to trigger the release of drug molecules from Au NP surfaces in numerous studies.[13−19] However, basic thermodynamic principles (endothermic vs exothermic behavior) suggest that molecular desorption is not guaranteed to happen upon heating, and that certain systems should exist in which heating causes further *adsorption* of molecules.

In this study, we use Le Chatelier's principle to predict and verify the adsorption and desorption of proteins to the functionalized surface of Au NPs.[20] We take advantage of the plasmon resonance of Au NPs to induce heating for the purposes of upsetting an established protein−particle equilibrium. Our studies demonstrate good predictability over protein adsorption and desorption depending on the thermodynamics of the protein/nanoparticle pair, as described by Le Chatelier's principle. Comparison of photothermal heating to conventional (water bath) heating suggests that while the trends observed for endothermic vs exothermic systems are in accord with the principle, quantitative differences between photothermal and conventional heating do occur. These observations suggest that nonequilibrium protein structures may occur at nanoparticle surfaces in complex media; but in terms of general protein adsorption or desorption to nanoparticle surfaces, LeChatelier's principle is found to provide a measure of predictability.

## RESULTS

In order to apply Le Chatelier's principle to protein adsorption to nanorods, we investigated the interactions of bovine serum albumin (BSA) and lysozyme (LYS) in the presence of either poly(allylamine hydrochloride) (PAH) or poly(vinyl sulfonate) (PVS) gold nanorods (Au NRs) to represent endothermic and exothermic systems, respectively. These pairs were selected based on previous studies that quantified the thermodynamics of their interactions.[21,22] The formation of protein/polyelectrolyte complexes can be written as follows, where Δ indicates heat:

$$\text{BSA} + \text{PAH} + \Delta \rightarrow \text{BSA/PAH complex (endothermic)}$$

$$\text{LYS} + \text{PVS} \rightarrow \text{LYS/PVS complex} + \Delta \text{ (exothermic)}$$

In an endothermic reaction, heat is supplied to the reactants in order to form the products, while the opposite is true of an exothermic reaction. If heat is added to an endothermic reaction at equilibrium, according to Le Chatelier's principle, the reaction should proceed to favor the formation of products (BSA/PAH complex). On the other hand, if heat is supplied to an exothermic reaction, regeneration of reactants should

Received: July 11, 2017
Published: September 18, 2017

  

DOI: 10.1021/acscentsci.7b00302
ACS Cent. Sci. 2017, 3, 1096−1102

**Scheme 1. Cartoon of the Expected Behavior of Proteins on Nanoparticle Surfaces Given the Thermodynamics of Each System**[a]

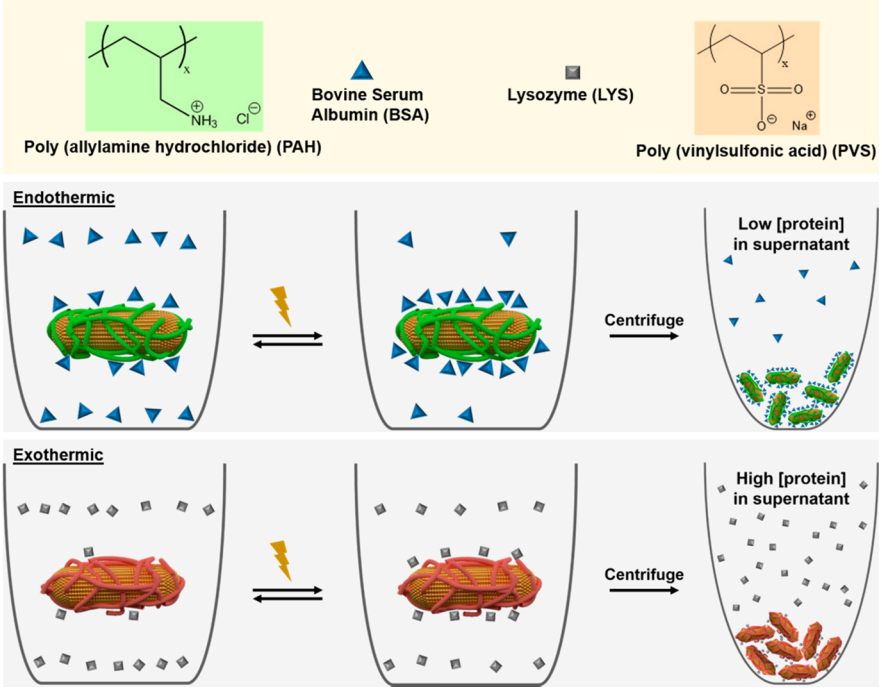


[a]The behavior is tested by measuring the protein concentration in the supernatant following centrifugation. Endothermic reactions favor the complex upon addition of heat and will contain less protein in the supernatant, while exothermic reactions favor free reactants, leading to higher protein concentration in the supernatant.

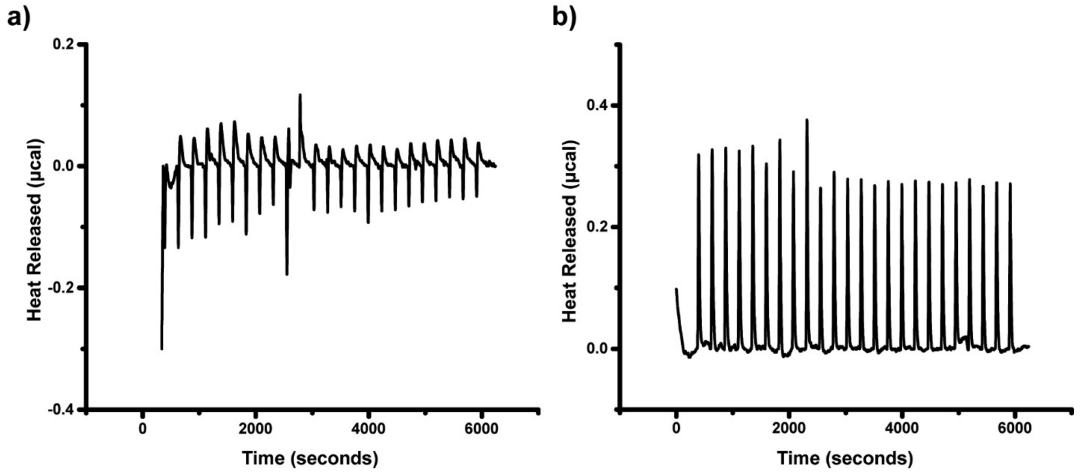


**Figure 1.** ITC titration curves of (a) 60 $\mu$M BSA to 14 nM PAH-wrapped Au NRs in 20 mM HEPES buffer at pH 7 (endothermic system) and (b) 60 $\mu$M LYS to 14 nM PVS-wrapped Au NRs in 20 mM HEPES buffer at pH 7 (exothermic system).

happen instead (LYS + PVS). These behaviors are summarized in Scheme 1.

Isothermal titration calorimetry (ITC) was used to confirm the endothermic/exothermic behavior of BSA + PAH and LYS + PVS (Figure S1). Furthermore, we determined that the wrapping of these polyelectrolytes around gold nanorods does not change the sign of the thermodynamics upon interactions with proteins (Figure 1). From the ITC titration data, we were also able to estimate an average $\Delta H$ for each system. For the addition of BSA to PAH-wrapped NRs, we calculate that $\Delta H$ = +3.22 kJ/mol, and when LYS was added to PVS-wrapped NRs, $\Delta H$ = −10.25 kJ/mol. As Au NRs are in excess under the ITC experimental conditions, $\Delta H$ values are reported in terms of moles of protein. Previous studies have calculated the $\Delta H$ for the interactions between BSA and PAH to be +400 kJ/mol, and −63.6 kJ/mol for LYS and PVS.[21,22]

Au NR solutions with a plasmon peak that overlapped the 808 nm laser wavelength were synthesized using a method developed by Zubarev and co-workers.[23] Laser irradiation of a 0.1 nM solution of Au NRs resulted in an increase of temperature to approximately 36 °C after 10 min (Figure S2), which acted as the heat source for our experiments. As the interaction between BSA and PAH-wrapped NRs is endothermic, we expect that, upon plasmonic heating, the system should favor complexation between BSA and PAH-wrapped NRs, and therefore less free BSA in the supernatant. To observe this



DOI: 10.1021/acscentsci.7b00302
ACS Cent. Sci. 2017, 3, 1096−1102

effect, BSA-coated PAH-wrapped Au NRs were subjected to 808 nm laser irradiation, and the amount of free BSA after removal of Au NRs by centrifugation was quantified using fluorescence as well as the BCA assay (Figures 2 and S3).

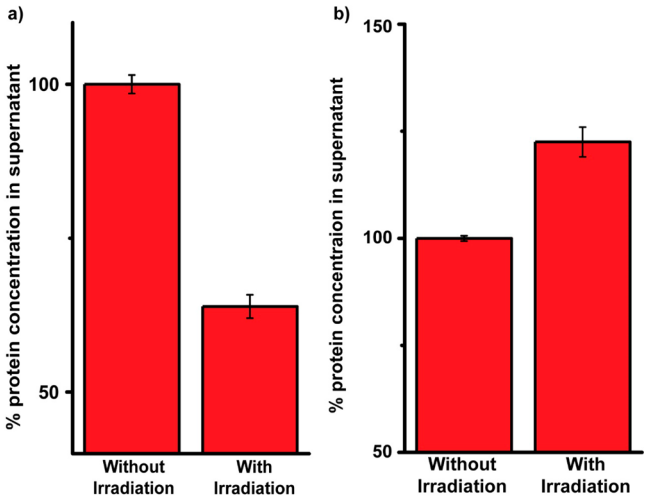


**Figure 2.** Percentage of protein remaining in the supernatant of (a) BSA−PAH Au NRs (endothermic system) and (b) LYS−PVS Au NRs (exothermic system) for 1 nM (in particles) of NIR-absorbing gold nanorods and 10 $\mu$M protein in 20 mM HEPES buffer, illuminated at the longitudinal plasmon band maximum of 808 nm for 5 min. Protein concentrations in the supernatants were measured according to fluorescence calibration curves, and the data shown are the averages of 5 replicates (error bars indicate one standard deviation). The samples not exposed to irradiation were set to 100%.

These concentrations were compared to samples consisting of BSA-coated PAH-wrapped Au NRs not exposed to laser irradiation. In at least five independent nonirradiated samples, the amount of free BSA remaining after removal of Au NRs was 0.374 ± 0.002 $\mu$M. However, in the samples exposed to laser irradiation, the amount of BSA remaining in the supernatant fell to 0.236 ± 0.001 $\mu$M, approximately 60% of the nonirradiated sample (Figure 2). Calculation of protein concentration using the BCA assay showed the same trend, with the amount of BSA found in the supernatants of laser-irradiated samples being only 50% compared to the samples not exposed to light. In this endothermic system, more BSA was bound to the Au NRs after laser irradiation compared to samples which were not exposed to laser irradiation.

According to Le Chatelier's principle, the behavior of an exothermic system should be opposite to our observations of an endothermic system, in that heat supplied to the system should drive the reaction toward formation of the reactants (decomplexation of LYS and PVS NRs). Using the same laser wavelength for plasmon excitation, we monitored the concentrations of LYS in the supernatant with and without exposure to laser irradiation. In the LYS/PVS NR solutions not exposed to laser irradiation, we observed a LYS concentration in the supernatant of 1.47 ± 0.078 $\mu$M LYS, while in the samples exposed to laser irradiation there was a LYS concentration in the supernatant of 1.82 ± 0.034 $\mu$M (Figures 2 and S3). This represents a 125% increase in LYS concentration in the supernatant when the exothermic complex is exposed to laser (Figure 2). Quantification of the supernatant LYS concentration using the BCA assay produced a similar result, which showed an increase in LYS concentration by 130% in samples exposed to laser irradiation. This exothermic pair showed the release of LYS from the NP surface, synonymous with the system shifting its equilibrium away from complexation as heat is applied.

Gold nanospheres (Au NSs) exhibiting the appropriate surface chemistries (PAH or PVS) were created as controls to highlight the importance of using an on-resonant laser wavelength. As the plasmon absorbance peak of Au NSs is significantly shifted away from the laser wavelength used to generate heat, we expect minimal heating to occur, and therefore should not observe the same thermodynamic responses when the samples are irradiated with a laser (Figure 3). When BSA−PAH Au NSs were irradiated with an 808 nm laser for 5 min, we found that 0.367 ± 0.004 $\mu$M BSA remained as free protein after centrifugation, as compared to 0.377 ± 0.003 $\mu$M BSA in the nonirradiated sample. Additionally, when the same experiment was repeated on LYS−PVS Au NSs, there was 1.06 ± 0.004 $\mu$M LYS remaining as free protein following laser irradiation, as compared to 0.90 ± 0.08 $\mu$M in the nonirradiated sample. However, when a water bath was used to heat the solutions, the amount of free protein in the BSA−PAH Au NSs solution decreased to 0.307 ± 0.001 $\mu$M BSA, and the amount of free protein in the LYS−PVS Au NSs sample increased to 1.15 ± 0.029 $\mu$M LYS. In the case of BSA−PAH Au NSs, heating with the water bath resulted in 81% of the original protein concentration remaining in solution, while in the case of LYS−PVS Au NSs, heating with the water bath resulted in an increase of the original protein concentration of 127% (Figure 3). These percentages are calculated with respect to samples not exposed to laser irradiation. Measurement of the protein content in the supernatant using the BCA assay yielded similar results: in BSA−PAH Au NS samples, only 90% of the original protein content was observed, while in LYS−PVS Au NS samples, we observed 120% of the original protein content.

To test how well LeChatelier's principle would predict protein−nanoparticle binding in a more realistic biological environment, similar experiments were performed using fluorphore-labeled proteins complexed with NPs incubated in 10% fetal bovine serum (FBS) (Scheme 2, Figure S4). The area under the fluorescence curve (at the excitation and emission of the respective dyes) of the supernatant was calculated as a representation of the amount of protein adsorbed to or released from the nanoparticle (Figure S5). A solution containing the endothermic system fluorescein labeled bovine serum albumin (FITC-BSA) complexed with PAH Au NRs in 10% FBS was centrifuged, and we found 0.458 ± 0.02 $\mu$M BSA remaining in the supernatant based on the fluorescence intensity of fluorescein. When the same solution was exposed to the same laser irradiation conditions as described earlier, the concentration of BSA in the solution decreased to 0.429 ± 0.03 $\mu$M. This corresponds to 94% of the protein found in the supernatant when laser irradiation is applied (Figure 4). The behavior of exothermic systems was tested under similar conditions by using rhodamine-B labeled lysozyme (RB-LYS) complexed with PVS-wrapped Au NRs. In the samples not exposed to laser illumination, we found a concentration of RB-LYS of 0.379 ± 0.006 $\mu$M based on fluorescence (Figure 4). Meanwhile, the supernatant of samples subjected to laser irradiation had an average RB-LYS concentration of 0.551 ± 0.003 $\mu$M. This represents an approximately 145% increase in protein concentration, similar to what is achieved when the sample is heated using a water bath (Figure S6). Monitoring of the heats absorbed and released by titrating FBS to PVS Au


DOI: 10.1021/acscentsci.7b00302
ACS Cent. Sci. 2017, 3, 1096−1102

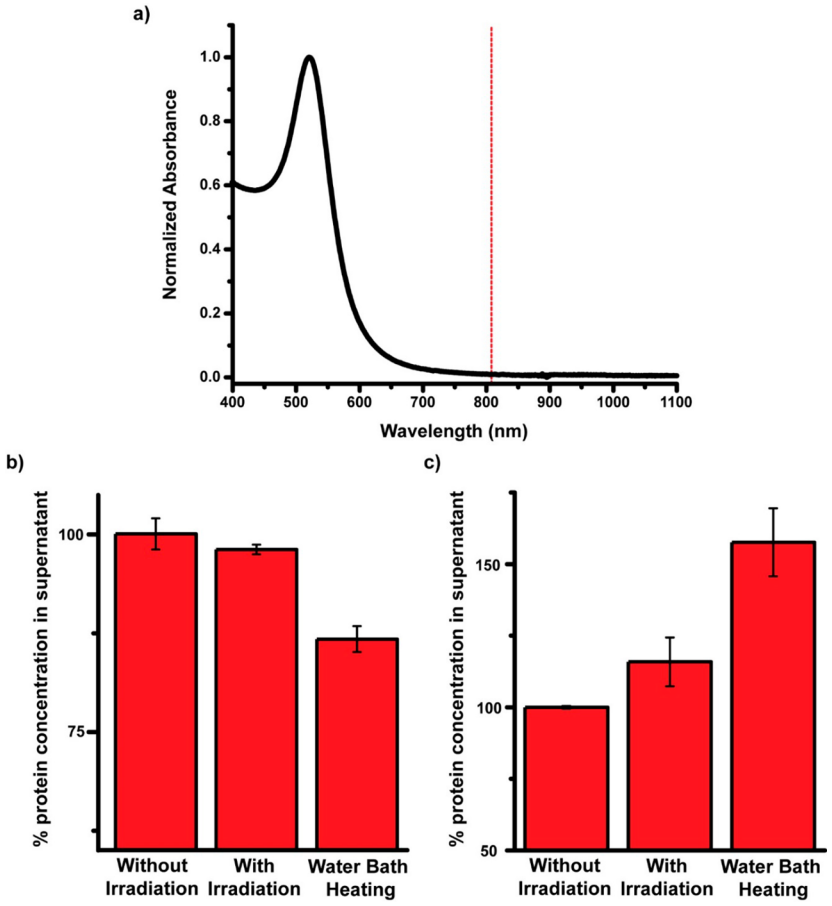


**Figure 3.** (a) Absorbance spectrum of 20 nm Au NSs. The 808 nm laser wavelength that is resonant for Au NRs is marked with a red dashed line. (b, c) Percentage of protein remaining in the supernatant of (b) the endothermic system BSA/PAH-wrapped NSs and (c) the exothermic system LYS/PVS-wrapped NSs for 1 nM (in particles) Au NSs and 10 $\mu$M protein in 20 mM HEPES buffer, illuminated at 808 nm for 5 min. Protein concentration in the supernatants was measured according to fluorescence calibration curves, and the data shown are the averages of 5 replicates (error bars indicate one standard deviation). The samples not exposed to irradiation were set to 100%.

**Scheme 2. Scheme of Expected RB-LYS Behavior When Attached to PVS Au NRs and Incubated in FBS, Given Previous Observations**[a]

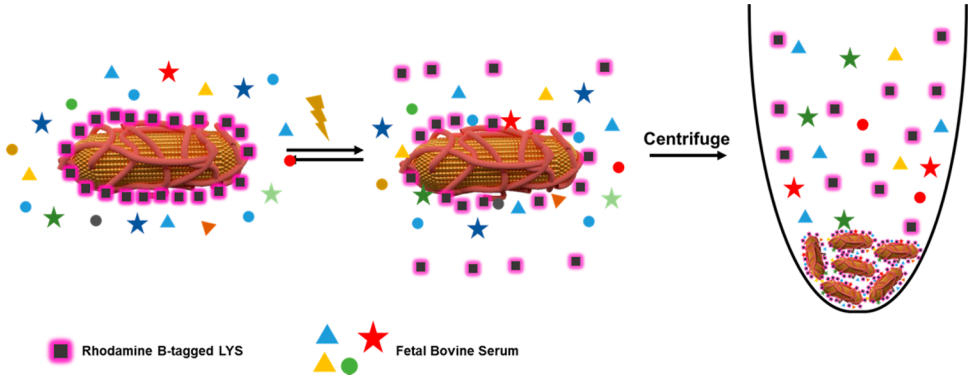


[a]As exothermic systems were shown to favor dissociation upon plasmonic irradiation, we expect there to be a higher amount of RB-LYS in the supernatant after centrifugation.

NRs using ITC showed no clear indication of either endothermic or exothermic behavior (Figure S7).

## DISCUSSION

In order to demonstrate Le Chatelier's principle for photothermal heating of gold nanorod systems, the appropriate surface chemistries for endothermic and exothermic complexations were required. Through their study of the complexation of protein bovine serum albumin (BSA) and the cationic polyelectrolyte poly(allylamine hydrochloride) (PAH), Schaaf and co-workers noted a positive binding enthalpy between BSA and PAH of 400 kJ/mol.[21] Romanini et al. calculated the binding enthalpy of the protein lysozyme to the anionic polyelectrolyte poly(vinyl sulfonic acid) (PVS) to be negative:


DOI: 10.1021/acscentsci.7b00302
ACS Cent. Sci. 2017, 3, 1096−1102

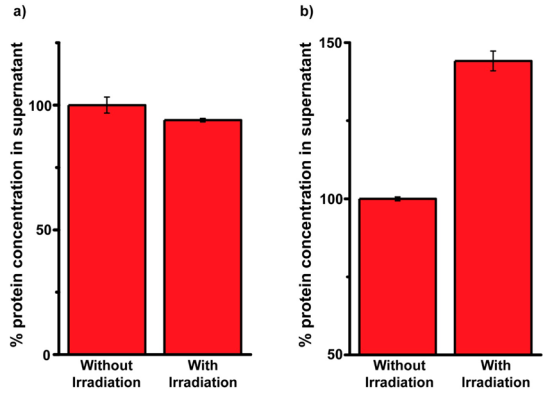


**Figure 4.** Percentage of protein remaining in the supernatant of (a) FITC-BSA and PAH NRs (endothermic) in 10% FBS and (b) RB-LYS and PVS NRs (exothermic) in 10% FBS as calculated from the fluorescence of the dye-labeled proteins. The sample not exposed to irradiation was set to 100%.

−63.6 kJ/mol.[22] In our own experiments, the $\Delta H$ values for the interactions between proteins and these polyelectrolytes wrapped around Au NRs (BSA/PAH Au NRs, $\Delta H$ = +3.22 kJ/mol; LYS/PVS Au NRs, $\Delta H$ = −10.25 kJ/mol) are significantly lower than these previously reported values for free polyelectrolyte, although the endothermic/exothermic nature of the binding remains the same. This could be caused by the fixation of polyelectrolytes to a surface, which can affect molecular binding and interactions. By using molecular dynamics simulations, noncovalent affinities between polymers were shown to increase upon increasing the flexibility of molecules.[24] Furthermore, Monte Carlo simulations revealed stronger binding of counterions as the rigidity of charged oligomers was decreased.[25] Although we have no direct experimental data regarding polyelectrolyte flexibility on curved surfaces, nor counterion binding to colloidal nanoparticles coated with polyelectrolytes compared to free polyelectrolytes, these molecular-level details from simulation support the notion that binding affinities and magnitude of enthalpies of polymer−protein interactions would be reduced upon polymer binding to a surface.

Having shown that the thermodynamics of the complexation of proteins and polyelectrolytes does not change sign upon wrapping the polyelectrolytes on nanoparticles, we chose to use the strong light absorption of Au NRs as an external heat source to shift the equilibrium of the system. When heat is added to an endothermic reaction, the equilibrium will shift to favor the product side, or in this case, the BSA/PAH complex. This means that the amount of free BSA in the supernatant after removal of NRs via centrifugation should decrease when compared to the sample that was not irradiated, which is exactly what is observed through fluorescence measurements and BCA protein assays. To further show the effects of Le Chatelier's principle on the nanoscale, the interaction of LYS and PVS-wrapped NRs was used as the exothermic model. Application of heat to this system will drive the reaction toward the product side, effectively releasing bound protein from the surface of the nanoparticle. Integration of fluorescence curves as well as results from the BCA assay agree show increased concentrations of free protein in the supernatant, in agreement with how an exothermic system would behave.

Au nanospheres were picked as an additional control condition due to their plasmon resonance, at 520 nm, being far away from 808 nm to reduce absorption of the laser light and therefore photothermal heating. Indeed, for the endothermic case (Figure 3), photothermal "heating" of off-resonant gold nanospheres leads to no change in protein complexation compared to the control. There is some effect in the exothermic case (Figure 3), although we note that (i) the enthalpy change is more significant here and (ii) there could be a small amount of light absorption even for spheres at 808 nm. When a water bath is used to heat the sample to 35 °C for 5 min, the expected Le Chatelier effects are observed: the endothermic system sequesters protein, and the exothermic system releases protein (Figure 3). This data might suggest that, in terms of the thermodynamics of protein adsorption, the surface chemistry plays a more important role than the shape or size of the particle.

Experiments in which the protein/NR complex was incubated in 10% FBS represent a model for an in vivo environment. Observation of Le Chatelier's principle dictating the adsorption and desorption of protein suggest that, even in a complex environment, specific interactions between single proteins and NPs can be predicted using this concept. The adsorption of FITC-BSA onto PAH-wrapped Au NR surfaces in 10% FBS was much less efficient than when a similar experiment was performed in 20 mM HEPES buffer, most likely due to the many proteins and growth factors present in FBS. The individual components of FBS could be competing for the NR surface, and furthermore, other constituents of FBS could also exhibit endothermic behavior when complexing with PAH. However, despite both of these considerations, there is still a slight increase of absorption of FITC-BSA to the NR surface upon laser irradiation. Conversely, the release of RB-LYS from the surface of PVS-wrapped NRs is more efficient than when the experiment is performed in aqueous buffer. This could be due to the same reasons which caused adsorption of FITC-BSA to the PAH NR surface to be difficult; in keeping with favorable thermodynamic interactions, certain endothermic pairs which favor complexation could likely force additional RB-LYS off of the PVS NR surface.

It has been previously shown by Suslick and co-workers that plasmonic heating of Au NRs by laser irradiation changes the content of the protein corona around nanoparticles, which can in turn change the biological fate of the NPs.[26] In their study, Au NRs coated with a cationic surfactant (CTAB) were incubated in 10% FBS and the NRs were subjected to irradiation at the longitudinal plasmon band maximum. Using liquid chromatography methods in conjunction with mass spectrometry, they were able to determine that, following laser heating, there were significant changes to the composition of the protein corona comparing laser-induced heating to no heating, and they also found more modest differences when comparing laser-induced heating to water-bath heating.[26] We observe similar results here: laser-induced heating does not give the same quantitative response as water-bath heating (in terms of protein adsorption or desorption) although, qualitatively, endothermic is endothermic and exothermic is exothermic. These data, taken together, suggest the interesting hypothesis that nonequilibrium protein structures exist at nanoparticle surfaces, which then alter protein−protein and protein−nanoparticle interactions. Nonetheless, even in a complex medium like FBS, LeChatelier's principle does successfully predict that an exothermic protein/NP combination does lead to protein desorption upon laser irradiation (Figure 4b), while an endothermic protein/NP combination does lead to (slight)


DOI: 10.1021/acscentsci.7b00302
ACS Cent. Sci. 2017, 3, 1096−1102

increased protein adsorption to the NPs and therefore less protein in the supernatant (Figure 4a).

## CONCLUSION

In this study, we have shown that Le Chatelier's principle can be applied on the nanoscale to predict the interactions between proteins and nanoparticles. We have demonstrated prediction and control of adsorption and desorption of specific proteins to polyelectrolyte-wrapped Au NPs by using laser-induced plasmonic heating based on Le Chatelier's principle. Additionally, we show that these results remain applicable even in a complex environment such as fetal bovine serum. The concepts presented here can be expanded to include a broader range of proteins and biomolecules in order to advance the management of the protein corona for nanoparticle therapeutic purposes. In addition, the concept that a trigger meant to release molecules (photothermal heating) might actually promote sequestration of molecules to NP surfaces (for endothermic NP−molecule systems) needs to be considered for furthering inquiry at the nano−bio interface.

## MATERIALS AND METHODS

All chemicals used in nanoparticle synthesis and functionalization (chloroauric acid, trisodium citrate, cetyltrimethylammonium bromide (CTAB), silver nitrate, sodium borohydride, hydroquinone, poly(allylamine hydrochloride) (PAH), HEPES, and poly(vinyl sulfonate) (PVS)) were purchased from Sigma-Aldrich and used without further purification. Lysozyme from chicken egg white was also purchased from Sigma-Aldrich, and bovine serum albumin (BSA) was purchased from Santa Cruz Biotechnology, Inc. Rhodamine B-tagged lysozyme (RB-LYS) was purchased from Nanocs. Fluorescein-labeled BSA (FITC-BSA) was obtained from Life Technologies. Nanoparticle concentrations were determined by measuring optical absorbance using a Cary 5000 UV−vis−NIR spectrophotometer using known extinction coefficients. Isothermal titration calorimetry (ITC) titrations were performed on a NanoITC (TA Instruments), and fluorescence spectra were taken with a Cary Eclipse fluorescence spectrophotometer.

**Synthesis of Citrate-Coated Nanospheres.** 20 nm citrate-coated gold nanospheres (Au NSs) were synthesized according to the Turkevich method.[27] Briefly, a solution of 97.5 mL of $H_2O$ and 2.5 mL of 0.01 M $HAuCl_4$ was stirred and brought to a rolling boil. Then, 2 mL of 5% wt solution of sodium citrate was added to begin the reduction process, and the solution was allowed to boil for 30 min. After 30 min, the heat was turned off, and the NPs were washed via centrifugation for 20 min at 8,000 rcf.

**Synthesis of Gold Nanorods.** Gold nanorods (Au NRs) were synthesized using methods published by Zubarev and coworkers.[23] Briefly, a seed solution was made by adding 0.46 mL of 0.01 M $NaBH_4$ in 0.01 M NaOH to a solution containing 0.5 mL of 0.01 M $HAuCl_4$ and 9.5 mL of 0.1 M CTAB. Next, a growth solution consisting of 9.5 mL of 0.1 M CTAB, 0.5 mL of 0.01 M $HAuCl_4$, and between 10 and 50 $\mu$L of 0.1 M $AgNO_3$ was prepared, to which 160 $\mu$L of seeds was added. The solutions were stored overnight to allow growth to reach completion, and cleaned via centrifugation for 20 min at 4,500 rcf.

**Polyelectrolyte Wrapping of Gold Nanoparticles.** Polyelectrolyte wrapping of nanoparticles was performed after one round of washing. 10 mL of 0.5 nM nanorods or 1 nM nanospheres was incubated with 1 mL of 0.01 M NaCl and 2 mL of 10 mg/mL poly(allylamine hydrochloride) (PAH) or poly(vinyl sulfate) (PVS), depending on the surface charge of the nanoparticle. The solutions were incubated overnight before removal of excess reactants via centrifugation under previously reported conditions.

**Isothermal Titration Calorimetry.** In all ITC experiments, the protein was loaded in the syringe as the titrant, and the polyelectrolytes/polyelectrolyte-wrapped nanoparticles were contained in the cell as the titrand. The titrand was kept in excess to avoid aggregation (polyelectrolyte concentration was at least 5 mg/mL, and polyelectrolyte-wrapped NR concentration was at least 14 nM), while the protein concentration in the syringe was 300 $\mu$M for titrations into polyelectrolyte solutions and 60 $\mu$M for titrations to Au NRs. A set of titrations consisted of 1 injection of 0.48 $\mu$L, followed by 24 injections of 2 $\mu$L each. Stirring was set to a rate of 150 rpm, and the cell temperature was kept at 25 °C.

**Preparation of Protein/NP Complexes.** To prepare protein/NP complexes, Au NRs (either PAH or PVS wrapped) were added to 10 mL of 10 $\mu$M protein (either BSA or LYS) as prepared in 20 mM HEPES buffer (pH 7) to a final NP concentration of 1 nM in particles, while stirring. The complexes was stored at 4 °C overnight and then centrifuged the following day to remove excess protein. For experiments involving FBS, the purified protein/NP complex was incubated in 10% FBS for one further night at 4 °C to allow the final equilibrium of the system to be reached.

**Quantification of Protein Concentration in the Supernatant.** Protein content was quantified using fluorescence measurements and the Micro BCA Protein Assay Kit (ThermoFisher, Catalog No.: 23235). Following laser irradiation for 5 min or water bath heating at 35 °C for 5 min, NP solutions were centrifuged for 5 min at 7,000 rcf, and the top 80 $\mu$L was removed and diluted to 680 $\mu$L for analysis. 650 $\mu$L of protein solutions were used for fluorescence measurements, and 500 $\mu$L of protein solutions were used for the Micro BCA Assay. For fluorescence measurements of unlabeled protein, the excitation wavelength was set at 280 nm, and emission spectra were collected from 300 to 400 nm. To measure the fluorescence of Rhodamine B labeled lysozyme (RB-LYS), the excitation was set at 540 nm, and the emission spectra were collected from 545 to 645 nm. Similarly, the concentration of fluorescein-labeled BSA (FITC-BSA) was determined by setting the excitation wavelength to 490 nm and collecting the emission spectra from 495 to 595 nm.

## ASSOCIATED CONTENT

### Supporting Information

The Supporting Information is available free of charge on the ACS Publications website at DOI: 10.1021/acscentsci.7b00302.

Raw fluorescence intensity data and ITC titration measurements (PDF)

## AUTHOR INFORMATION

### Corresponding Author

*E-mail: murphycj@illinois.edu. Phone: +1 217 333-7680. Fax: +1 217 244-3186.

### ORCID

Catherine J. Murphy: 0000-0001-7066-5575

### Notes

The authors declare no competing financial interest.



DOI: 10.1021/acscentsci.7b00302
ACS Cent. Sci. 2017, 3, 1096−1102

## ■ ACKNOWLEDGMENTS

We thank S. Nitya Sai Reddy and Wenjing Wang of the Lu Research Group for their help in the laser irradiation experiments, Varun Mohan of the Jain Research Group for his help with fluorometer measurements, and Jennifer Hou of the Burke Group for her help in the ITC titrations. This work was supported by NSF Grants CHE-1608743 and 1306596.

## ■ REFERENCES

(1) Ghosh, P.; Han, G.; De, M.; Kim, C. K.; Rotello, V. M. Gold Nanoparticles in Delivery Applications. *Adv. Drug Delivery Rev.* **2008**, *60* (11), 1307−1315.
(2) Jain, S.; Hirst, D. G.; O'Sullivan, J. M. Gold Nanoparticles as Novel Agents for Cancer Therapy. *Br. J. Radiol.* **2012**, *85* (1010), 101−113.
(3) Mackey, M. A.; Ali, M. R. K.; Austin, L. A.; Near, R. D.; El-Sayed, M. A. The Most Effective Gold Nanorod Size for Plasmonic Photothermal Therapy: Theory and In Vitro Experiments. *J. Phys. Chem. B* **2014**, *118* (5), 1319−1326.
(4) Li, N.; Zhao, P.; Astruc, D. Anisotropic Gold Nanoparticles: Synthesis, Properties, Applications, and Toxicity. *Angew. Chem., Int. Ed.* **2014**, *53* (7), 1756−1789.
(5) Alkilany, A. M.; Murphy, C. J. Toxicity and Cellular Uptake of Gold Nanoparticles: What We Have Learned so Far? *J. Nanopart. Res.* **2010**, *12* (7), 2313−2333.
(6) Dubois, L. H.; Nuzzo, R. G. Synthesis, Structure, and Properties of Model Organic Surfaces. *Annu. Rev. Phys. Chem.* **1992**, *43*, 437−463.
(7) Indrasekara, A. S. D. S.; Wadams, R. C.; Fabris, L. Ligand Exchange on Gold Nanorods: Going Back to the Future. *Part. Part. Syst. Charact.* **2014**, *31* (8), 819−838.
(8) Smith, A. M.; Marbella, L. E.; Johnston, K. A.; Hartmann, M. J.; Crawford, S. E.; Kozycz, L. M.; Seferos, D. S.; Millstone, J. E. Quantitative Analysis of Thiolated Ligand Exchange on Gold Nanoparticles Monitored by $^{1}$H NMR Spectroscopy. *Anal. Chem.* **2015**, *87* (5), 2771−2778.
(9) Eustis, S.; El-Sayed, M. A. Why Gold Nanoparticles Are More Precious than Pretty Gold: Noble Metal Surface Plasmon Resonance and Its Enhancement of the Radiative and Nonradiative Properties of Nanocrystals of Different Shapes. *Chem. Soc. Rev.* **2006**, *35* (3), 209−217.
(10) Dobrovolskaia, M. A.; Patri, A. K.; Zheng, J.; Clogston, J. D.; Ayub, N.; Aggarwal, P.; Neun, B. W.; Hall, J. B.; McNeil, S. E. Interaction of Colloidal Gold Nanoparticles with Human Blood: Effects on Particle Size and Analysis of Plasma Protein Binding Profiles. *Nanomedicine* **2009**, *5* (2), 106−117.
(11) Walkey, C. D.; Olsen, J. B.; Song, F.; Liu, R.; Guo, H.; Olsen, D. W. H.; Cohen, Y.; Emili, A.; Chan, W. C. W. Protein Corona Fingerprinting Predicts the Cellular Interaction of Gold and Silver Nanoparticles. *ACS Nano* **2014**, *8* (3), 2439−2455.
(12) Dobrovolskaia, M. A.; Neun, B. W.; Man, S.; Ye, X.; Hansen, M.; Patri, A. K.; Crist, R. M.; McNeil, S. E. Protein Corona Composition Does Not Accurately Predict Hematocompatibility of Colloidal Gold Nanoparticles. *Nanomedicine* **2014**, *10* (7), 1453−1463.
(13) Huschka, R.; Zuloaga, J.; Knight, M. W.; Brown, L. V.; Nordlander, P.; Halas, N. J. Light-Induced Release of DNA from Gold Nanoparticles: Nanoshells and Nanorods. *J. Am. Chem. Soc.* **2011**, *133* (31), 12247−12255.
(14) Paasonen, L.; Laaksonen, T.; Johans, C.; Yliperttula, M.; Kontturi, K.; Urtti, A. Gold Nanoparticles Enable Selective Light-Induced Contents Release from Liposomes. *J. Controlled Release* **2007**, *122* (1), 86−93.
(15) Barhoumi, A.; Huschka, R.; Bardhan, R.; Knight, M. W.; Halas, N. J. Light-Induced Release of DNA from Plasmon-Resonant Nanoparticles: Towards Light-Controlled Gene Therapy. *Chem. Phys. Lett.* **2009**, *482* (4−6), 171−179.
(16) Huang, J.; Jackson, K. S.; Murphy, C. J. Polyelectrolyte Wrapping Layers Control Rates of Photothermal Molecular Release from Gold Nanorods. *Nano Lett.* **2012**, *12* (6), 2982−2987.
(17) Liu, J.; Maaroof, A. I.; Wieczorek, L.; Cortie, M. B. Fabrication of Hollow Metal "Nanocaps" and Their Red-Shifted Optical Absorption Spectra. *Adv. Mater.* **2005**, *17* (10), 1276−1281.
(18) Bakhtiari, A. B. S.; Hsiao, D.; Jin, G.; Gates, B. D.; Branda, N. R. An Efficient Method Based on the Photothermal Effect for the Release of Molecules from Metal Nanoparticle Surfaces. *Angew. Chem., Int. Ed.* **2009**, *48* (23), 4166−4169.
(19) Pissuwan, D.; Valenzuela, S. M.; Cortie, M. B. Therapeutic Possibilities of Plasmonically Heated Gold Nanoparticles. *Trends Biotechnol.* **2006**, *24* (2), 62−67.
(20) Le Chatelier, H. L. Les Equilibres Chimiques. *Ann. Mines* **1888**, *13*, 157−382.
(21) Ball, V.; Winterhalter, M.; Schwinte, P.; Lavalle, P.; Voegel, J.-C.; Schaaf, P. Complexation Mechanism of Bovine Serum Albumin and Poly(allylamine Hydrochloride). *J. Phys. Chem. B* **2002**, *106* (9), 2357−2364.
(22) Romanini, D.; Braia, M.; Angarten, R. G.; Loh, W.; Picó, G. Interaction of Lysozyme with Negatively Charged Flexible Chain Polymers. *J. Chromatogr. B: Anal. Technol. Biomed. Life Sci.* **2007**, *857* (1), 25−31.
(23) Vigderman, L.; Zubarev, E. R. High-Yield Synthesis of Gold Nanorods with Longitudinal SPR Peak Greater than 1200 nm Using Hydroquinone as a Reducing Agent. *Chem. Mater.* **2013**, *25* (8), 1450−1457.
(24) Forrey, C.; Douglas, J. F.; Gilson, M. K. The Fundamental Role of Flexibility on the Strength of Molecular Binding. *Soft Matter* **2012**, *8* (23), 6385−6392.
(25) Sajevic, T.; Rescic, J.; Vlachy, V. Correlation between Flexibility of Chain-like Polyelectrolyte and Thermodynamic Properties of Its Solution. *Condens. Matter Phys.* **2011**, *14* (3), 33603.
(26) Mahmoudi, M.; Lohse, S. E.; Murphy, C. J.; Fathizadeh, A.; Montazeri, A.; Suslick, K. S. Variation of Protein Corona Composition of Gold Nanoparticles Following Plasmonic Heating. *Nano Lett.* **2014**, *14* (1), 6−12.
(27) Turkevich, J.; Stevenson, P. C.; Hillier, J. A Study of the Nucleation and Growth Processes in the Synthesis of Colloidal Gold. *Discuss. Faraday Soc.* **1951**, *11*, 55−75.



DOI: 10.1021/acscentsci.7b00302
*ACS Cent. Sci.* 2017, 3, 1096−1102